

RF Response of Single-Walled Carbon Nanotubes

Luis Gomez-Rojas, Somnath Bhattacharyya,[†] Ernest Mendoza, David C. Cox, J. Mauricio Rosolen,[‡] and S. Ravi P. Silva*

Nano-Electronics Centre, Advanced Technology Institute, University of Surrey, Guildford GU2 7XH, United Kingdom

Received May 6, 2007

ABSTRACT

We present for the first time an in-depth study of the RF response of a single-walled carbon nanotube (SWCNT) rope. Our novel electrode design, based on a tapered coplanar approach, allows for single tube measurements well into the GHz regime, minimizing substrate-related parasitics. From the analysis of the S-parameters, the ac transport mechanism in the range 30 kHz to 6 GHz is established. This work is an essential prerequisite for the fabrication of high-speed devices based on bundles of nanowires or low-dimensional structures.

Semiconducting single-walled carbon nanotubes (SWCNTs) have shown huge potential for integrated circuits on a scale smaller than that achieved by silicon.^{1–6} However, in order to fully exploit the advantages of SWCNTs, a thorough study of their dynamic properties, beyond the sub-GHz range,¹ is needed. Theoretical work has postulated high-frequency properties of nanotubes, which in turn has created a push for an intensive study into the GHz regime.^{7–10} On the basis of the high-speed switching properties of nanotubes, a route to a new class of integrated circuits has been made possible, with interconnects, memory, nanoelectromechanical, and other large-area applications all now within the scope of this system.^{1–7} As a first step, we have recently demonstrated fast switching (GHz range) in two-dimensional and filamentary structures of amorphous carbon.¹¹ However, for nanotube-based systems, high-frequency performance is yet to be fundamentally understood.² To this end, several attempts for investigating transmission performance of CNTs at GHz frequencies have been proposed.^{6–9,12} Some of the major problems in characterizing nanotubes in the GHz regime are the very small signal levels and the presence of parasitics inherent to all nanosystems.¹² All these methods, although innovative, have not delivered the unambiguous measurement of a single nanotube characteristics in the GHz regime; moreover, an in depth analysis of the complex impedance of a single rope is still not reported. Although there have been some reports at low frequencies (MHz)¹³ and THz regime,¹⁴ an analysis of complex impedance in the GHz

regime, crucial for potential applications of CNTs in today's commercial systems,⁸ has yet to be reported. In the GHz regime, even though there have been some theoretical predictions of the features related to the response of conduction electrons, 1-D plasmon, and Luttinger liquid behavior in SWCNTs, the experimental verification has proven to be difficult.^{7,15,16}

In this Letter, we present the full RF characterization (30 kHz to 6 GHz) of a single SWCNT rope by means of a novel approach based on a tapered coplanar topology. The method allows for high-frequency measurements well into the GHz regime, minimizing the effects of parasitic capacitance due to the proximity between electrodes, capacitive losses due to coupling through the dioxide layer to the substrate,⁷ and allowing for single nanotube characterization due to the shape of the electrodes. We investigate the carrier transport mechanism and the dielectric relaxation in this CNT rope and determine the crucial parameters for understanding the high-frequency response in this system.

To minimize substrate-related parasitics present in Si substrates, 1 mm thick pure quartz was chosen for the experiment. For the coplanar electrode design and simulation, Advanced Design System (ADS) software was used, taking into consideration the substrate's intrinsic properties and the thin double-layered metal deposited in the substrate required for the nanotube's positioning on the electrodes. A through transmission line configuration and one with a small gap in the center conductor were designed and simulated. The fabrication was carried out in two stages: a thin layer of chromium (~3 nm), followed by a 40 nm layer of gold, was deposited onto the wafer by dc sputtering and the electrodes patterned by standard photolithography. Taking into consideration the tolerances in the photolithographic process, the

* Corresponding author. E-mail: s.silva@surrey.ac.uk. Telephone: +44-(0) 1483 689825.

[†] Permanent address: School of Physics, University of the Witwatersrand, P/Bag 3, Wits 2050, Johannesburg, South Africa.

[‡] Permanent address: Universidade de São Paulo, FFCLRP-DQ, Ribeirão Preto SP C.E.P. 14040-901, Brazil.

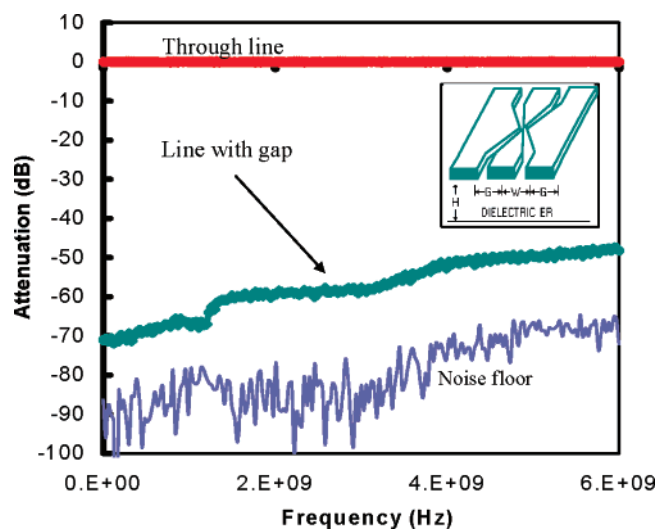


Figure 1. Measured S-parameters S21 for the electrode layout designed for CNT characterization.

through transmission line was fabricated and measured. The structure was then placed under a focused ion beam (FIB) and trimmed to form the electrode, creating a gap down to a resolution better than 100 nm and a separation of approximate 1 μm , and then the structure was measured again. Low loss better than 0.5 dB was obtained for the through line, while an isolation of better than 50 dB was obtained for the electrodes with the gap, which resulted in a negligible parasitic coupling contribution in our intended measured signal. Figure 1 shows the transmission characteristics for the electrodes designed and fabricated for this experiment.

The preparation of the CNT was made by ac dielectrophoresis, which involves the deposition of CNTs from solution by applying an alternating electric field between the electrodes. The frequency chosen was 10 MHz, which has been proven to attract predominantly metallic SWCNTs.¹⁷ A 0.5 μL drop of ultrapure 1,2-dichloroethane solution of SWCNT was placed between the electrodes, while an ac voltage of 10 Vp-p at 10 MHz was applied, attracting the SWCNTs in the solution toward the electrodes. The SWCNTs used in this study were grown by the arc discharge method using iron, nickel, and cobalt powders (~ 100 mesh, 99.99% Alfa Products) in a 1:1:1 molar proportion using a high-purity graphite rod (SGL Carbon Group) to initiate the arc. The SWCNTs were subject to purification before the dispersion in 1,2-dichloroethane. Analyses of SWCNTs under HRTEM (JEOL JEM 3010 at 300 kV) show open-ended SWCNTs with diameters in the range of 1.38–1.41 nm, as shown in Figure 2a.

Figure 2a shows that the samples studied are free of amorphous carbon and defects on the walls, impurities which can change the electronic properties of the sample and influence the environment such as interactions with oxygen. The sample was then diluted in a 1,2-dichloroethane solution and sonicated for 30 min before being deposited onto the substrate using dielectrophoresis, resulting in a single rope being attached between the electrodes, as verified by electron microscopy. An AFM analysis (shown on the inset of Figure

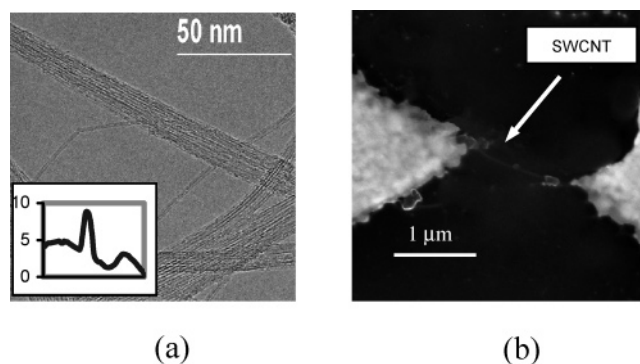


Figure 2. (a) High-resolution electronic microscopy of SWCNT used in this experiment. The inset in (a) shows a cross-sectional AFM scan of the height distribution in nm. (b) SEM micrograph of a single-walled carbon nanotube rope between metal electrodes.

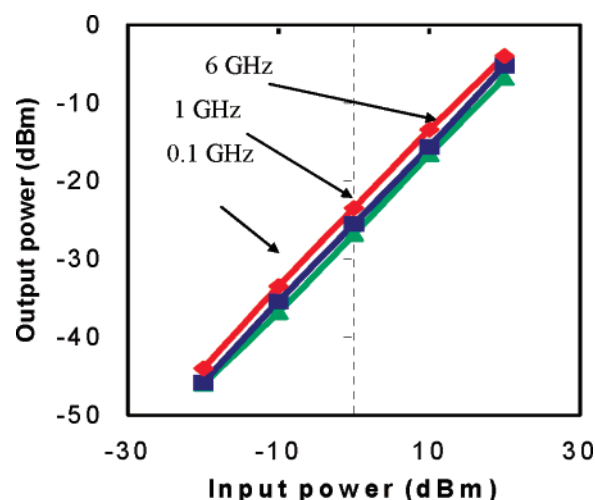


Figure 3. RF output power vs input power for nanotube bundle.

2a) of the tested CNTs revealed the bundle to consist of only a three-SWCNT rope sitting across the electrodes, as illustrated in Figure 2b.

Because of the physical dimensions of the nanotubes and the high contact resistance usually associated with nanotube connections (few k Ω s), the level of the signal into the input of standard high-frequency measurement equipment tends to be very small, making it difficult to separate out the signal from noise.¹ In our measurements, special care was taken to maximize the signal-to-noise ratio. To characterize the measurement system fully, we evaluated the dynamic range and the power handling capabilities in RF, using an HP-83623B signal generator, a portable probe station with 100-pitch coplanar probes, and an HP-8563B spectrum analyzer. Results showed a linear behavior over 20 dB at different frequencies (Figure 3) and a dynamic range of better than 40 dB for a 0 dBm input signal, which demonstrates that the current carrying capacity/capability of carbon nanotubes does not degrade with frequency well into the GHz regime and in agreement with that reported by Yu et al.¹⁰ Also, the relative rate ($P_{\text{in}}/P_{\text{out}}$) does not change at different frequencies, which is indicative of negligible parasitic coupling due to the tailored electrode configuration.

The sample was then characterized using a Vector network analyzer HP 4753E. A 0 dBm RF signal and an intermediate

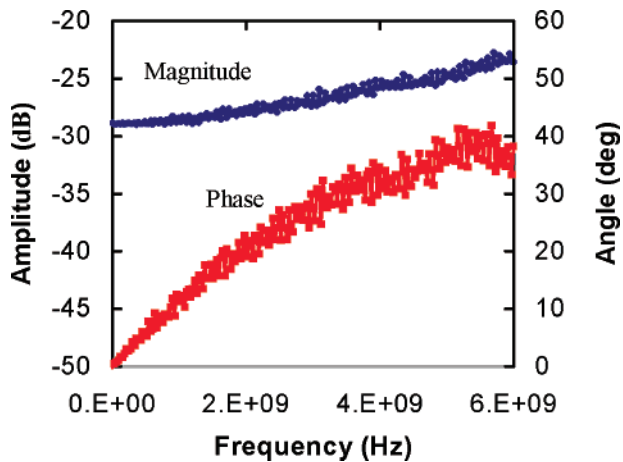


Figure 4. Measured S-parameter of SWCNT; plot in dB of transmitted power vs frequency.

frequency (IF) bandwidth of 300 Hz were used to ensure the noise floor of the instrument remained 40 dB below the measured signal to achieve less than 0.1 dB magnitude error and less than 0.6 dB phase error as recommended by the manufacturer. The system was accurately calibrated to 50 Ω . Figure 4 shows the S-parameters S21 for the sample shown in Figure 2 as a function of frequency from 0–6 GHz.

From the data, a relatively high transmission loss between –28 and –24 dB along the whole spectrum is apparent. In the lower part of the spectrum, this reflects an equivalent parallel quantum resistance of ~ 2.25 k Ω , which translates into an equivalent 6.75 k Ω (considering three tubes in parallel) close to the quantum limit reported in the literature,⁷ suggesting that the tubes are working in the quasiballistic state even at room temperature at high frequencies. However, the response also shows a gentle positive slope along the whole measured spectrum. As explained below, this is mainly caused by the influence of the nanotube's inherent capacitance with frequency, as estimated using the model proposed by Zhang et al.¹² and verified by simulation (not shown here).

From the reflected power (S11), using the standard relation $Z = (50 - S11)/(50 + S11)$, the equivalent system's impedance can be directly calculated as shown in Figure 5 and the system's equivalent electrical components that describe its behavior in high-frequency extracted.

A combined analysis of the data in Figures 4 and 5 can then be utilized to derive the capacitance and resistance of the tube(s) examined. A value of 15 fF for the capacitance and a value of 2.7 k Ω for the resistance is thus obtained from the complex impedance of the nanotube bundle. Parasitic capacitance due to electrode topology (fringe capacitance between electrode tips) was also calculated from our measurements. A value for the parasitics is found to be an order of magnitude less (~ 1.5 fF) than that calculated for the nanotube bundle. Hence, because our sample consists of three nanotubes in the rope measured, the equivalent capacitance per tube is estimated at 5 fF. The value is mainly dominated by the contact capacitance, which can be estimated as an electrostatic capacitance between a wire and a ground plane as reported by Burke⁷ given by $C_E = 2\pi\epsilon\ln(h/d)$, where h is the distance to the ground plane and d the diameter

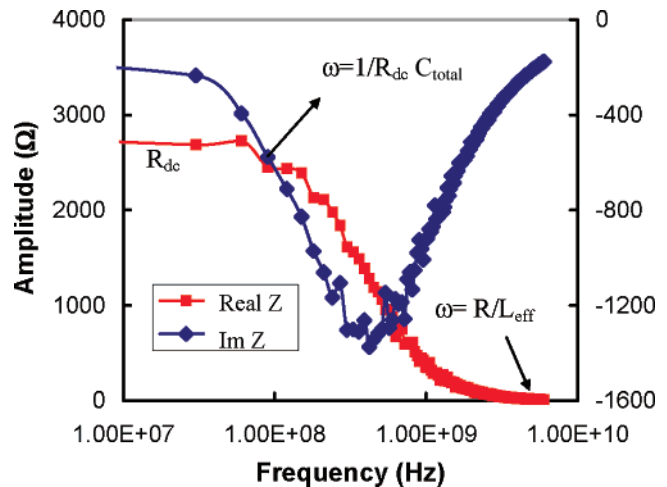


Figure 5. Impedance vs frequency of single-walled CNT bundle.

of the nanotube. Considering an average distance equal to the bundle diameter, a contact capacitance of several picofarads is more than an order of magnitude larger than that measured for our nanotube's sample. We do not see any strong evidence for negative quantum capacitance or kinetic inductance (characterized by the presence of a positive value of the imaginary part of the equivalent impedance Z) in the frequency range, unlike that proposed in previous reports.^{7,13}

Extrapolating the resistance of 2.7 k Ω was done by following the thorough analysis by Burke et al.⁷ Although, ballistic has not been claimed in this article, we have seen ballistic conductance at higher frequencies not presented in the present work. Burke explained the HF response by using the Luttinger liquid model, including plasmon oscillation and coherence length. What was sought in the article was experimental verification of those theoretically predicted values.

To understand and design devices for useful circuits, a technique needed to be developed to measure the frequency response in the 1-D plasmon velocity by exciting the 1-D plasmon using a microwave signal and establishing the validity of a Luttinger liquid model for SWCNTs.⁷ A damping mechanism of 1-D plasmon waves along the length of the tube was thought to describe the resistance of the system, which ultimately would give a value for the relaxation time (in ps). The length associated with this decay (l_{decay}) compared well to the length of the SWCNT and plays a significant role in the frequency response. Although we have not found a strong resonant peak, which would occur only if $l_{\text{decay}} > L_{\text{SWCNT}}$, the roll off of $\text{Re}(Z)$ with frequency has been recorded as predicted in the previous report and attributed to the overdamping of 1-D plasmons in SWCNTs (see Figure 5).⁷ Following ref 7, we derive the values for the effective CR time constant at 100 MHz and the L/R time constant at 2 GHz. The value for l_{decay} is estimated to be of the order of 10 nm (assuming the resistance per unit length is about 10 k $\Omega/\mu\text{m}$), which is much less than the length of the tube L (~ 800 nm). Because $l_{\text{decay}} < L_{\text{SWCNT}}$, no resonant behavior was observed in our measurement, establishing plasmons over damping.

The characteristic length (l_{mfp}) and time (τ) of a SWCNT has been determined from the dc resistance measured at low frequency and using the relationship $R_{\text{dc}} = (h/4e^2)(L/l_{\text{mfp}})$, where the value of l_{mfp} of 1.1 μm is suitable to support a ballistic-type conductance process in the present system. Assuming the Fermi velocity as $\sim 10^6\text{m/s}$, an estimated value of the relaxation time of several ps will allow for the cutoff frequency of the SWCNTs to go beyond a limit of 100 GHz.

The overall trend of S21 (magnitude and phase) has similarities to that reported by Zhang et al.,¹² confirming the accuracy of our measurement technique. However, the plot of $\text{Re}(Z)$ and $\text{Im}(Z)$ show that the transport mechanism in this system is substantially different from what was previously thought.¹² They¹² measured the current transport mechanism in this frequency range. Figure 5 shows the calculated system's impedance $\text{Re}(Z)$ and $\text{Im}(Z)$. From the plot, it is clear that $\text{Re}(Z)$ decays smoothly with frequency. On the other hand, the $\text{Im}(Z)$ shows a distinct minimum at about 0.5 GHz. This trend clearly shows a deviation from an ideal metallic tube. In our system, SWCNTs are mostly metallic, and electron-electron collision should be the dominant transport mechanism with a relaxation time of a few picoseconds.¹⁸

From this high electronic relaxation time, we can show the high-frequency application of the SWCNTs. However, for a bundle of SWCNTs due to its poor interconnectivity (and also empty air space), the frequency dependence would deviate from the ideal Drude's model for metals.¹⁴ This is confirmed by a distinct minimum at about 0.5 GHz, which is consistent with Wu et al.¹⁹ Several references show dielectric properties of CNTs from spectroscopic analysis, including HF, where effective medium theory can still be useful for a rope of CNTs without the presence of a composite.²¹ In this bundle of SWCNT, interconnections of tubes and effects of disorder (defects) can be summed up and the data treated as an effective medium. Therefore, in addition to the transport of conduction electrons through the single tube (relaxation time $\sim\text{fs}$), we can see dielectric relaxation effects (relaxation time $\sim\text{ps}$). Also, the effective permittivity of these samples show a resonance peak at 1.5 GHz, which signifies the Lorentzian oscillator term and a contribution from phonon of the system.¹⁴ Hence, we establish a very fast response system even though disorder and other effects may interfere and reduce any coherence within the structure measured. The corresponding time of 500 MHz ($\sim 0.2\text{ ns}$) is much smaller than those observed in commercial materials such as silicon nanostructures.²⁰ By considering that the electronic relaxation¹⁵ is the only transport mechanism, a very low value of capacitance of a few femtoseconds is confirmed. Based on this, we measure a GHz response for SWCNTs and is at a much higher frequency range than previously reported.⁷

In summary, we have introduced a new technique for high-frequency characterization of single-walled carbon nanotubes that falls within the frequency range of today's commercial communication technology. The method presented here allows for full ac characterization, minimizing the effects of parasitic coupling and substrate losses and the extraction

of relevant parameters for the application of nanotubes into future nanoelectronic or nanoelectromechanic systems. By employing this experimental technique, we can gain an understanding of the carrier transport mechanism of a single SWCNT bundle. No evidence for Luttinger liquid behavior or other quantum effects are found, which is consistent with previous experimental reports.⁷

Acknowledgment. This work is funded by the EPSRC's Portfolio Partnership Award. J. M. Rosolen thanks the CAPES-Brazil for a sabbatical fellowship. We also thank L. A. Montoro for HRTEM support and the LNLS.

References

- (1) Chen, Z.; Appenzeller, J.; Yu-Ming, L.; Sippel-Oakley, J.; Rinzler, A. G.; Tang, J.; Wind, J. S.; Solomon, P. M.; Avouris, P. *Science* **2006**, *311*, 1735.
- (2) Li, S.; Yu, Z.; Yen, S. F.; Tang, W. C.; Burke, P. J. *Nano Lett.* **2004**, *4*, 753–756. Yu, Z.; Rutherglen, C.; Burke, P. J. *Appl. Phys. Lett.* **2006**, *88*, 233115-3.
- (3) Feher, L.; Thumm, M.; Drechesler, K. *Adv. Eng. Mater.* **2006**, *8*, 26. Singh, D. V.; Jenkins, K. A. 63rd Device Research Conference, University of Notre Dame, South Bend, Indiana, June 21–23, 2004; pp 53–54.
- (4) Tans, S. J.; Alwin, R. M.; Verschuere, C.; Dekker, C. *Nature* **1998**, *393*, 393.
- (5) Pesetski, A. A.; Baumgardner, J. E.; Folk, E.; Przybysz, J. X.; Adam, J. D.; Zhang, H. *Appl. Phys. Lett.* **2006**, *88*, 113103-3.
- (6) Frank, D. J.; Appenzeller, J. *IEEE Electron Dev. Lett.* **2004**, *25*, 34–36; Singh, D. V.; Jenkins, K. A.; Appenzeller, J.; Neumayer, D.; Grill, A.; Wong, H. S. P. *IEEE Trans. Nanotechnol.* **2004**, *3*, 383–387.
- (7) Burke, P. J. *IEEE Trans. Nanotechnol.* **2002**, *1*, 129–144; **2003**, *2*, 55–58. Burke, P. J. *Solid State Electron.* **2004**, *48*, 1981–1986. Li, S.; Yu, Z.; Gaddie, G.; Burke, P. J.; Tang, W. C. *Proceedings of the 3rd IEEE Conference on Nanotechnology*, August 12–14, 2003; Vol. 1, pp 256–258. Yen, S. F.; Lais, H.; Yu, Z.; Li, S.; Tang, W. C.; Burke, P. *Proceedings of the 1st International Conference on Nanotechnology*, Singapore, July 13–17, 2004.
- (8) Teo, K. B. K.; Minoux, E.; Hudanski, L.; Peauger, F.; Schnell, J. P.; Gangloff, L.; Legagneux, P.; Dieumegard, D.; Amarantunga, G. A. J.; Milne, W. I.; *Nature* **2005**, *437*, p 968.
- (9) Kim, J.; So, H.-M.; Kim, N. *Phys. Rev. B* **2004**, *70*, 153402.
- (10) Yu, Z.; Burke, P. J. *Nano Lett.*, **2005**, *5*, 1403–1406; Burke, P. J.; Yu, Z.; Rutherglen, C. *Proceedings of the European Microwave Week*, Paris, October 3–7, 2005.
- (11) Bhattacharyya, S.; Henley, S. J.; Mendoza, E.; Gomez-Rojas, L.; Allam, J.; Silva, S. R. P. *Nat. Mater.* **2006**, *5*, 19–22.
- (12) Zhang, M.; Huo, X.; Liang, Q.; Tang, Z. K.; Chang, P. C. H.; *Proceedings of the 4th IEEE Conference on Nanotechnology*, Munich, August 16–19, 2004; Vol. 107, p 10. Zhang, M.; Huo, X.; Chan, P. C. H.; Liang, Q.; Tang, Z. K. *Appl. Phys. Lett.* **2006**, *88*, 163109.
- (13) Zhao, Y.-P.; Wei, B. Q.; Ajayan, P. M.; Ramamath, G.; Lu, T.-M.; Wang, G.-C.; Rubio, A.; Roche, S. *Phys. Rev. B* **2001**, *64*, 201402.
- (14) Jeon, T.; Son, J.; An, K. H.; Lee, Y. H.; Lee, Y. S.; *J. Appl. Phys.* **2005**, *98*, 034316.
- (15) Slepian, G. Y.; Shuba, M. V.; Maksimenko, S. A.; Lakhtakia, A. *Phys. Rev. B* **2006**, *73*, 195416.
- (16) Perfetti, L.; Kampfrath, T.; Schapper, F.; Gagen, A.; Hertel, T.; Aguirre, C. M.; Desjardins, P.; Martel, R.; Frischkorn, C.; Wolf, M. *Phys. Rev. Lett.* **2006**, *96*, 027401-4.
- (17) Mureau, N.; Mendoza, E.; Silva, S. R. P.; Hoettges, K. F.; Hughes, M. P. *Appl. Phys. Lett.* **2006**, *88*, 243109-3.
- (18) Dragoman, D.; Dragoman, M. *J. Appl. Phys.* **2006**, *99*, 076106.
- (19) Wu, J.; Kong, L. *Appl. Phys. Lett.* **2004**, *84*, 4956.
- (20) Axelrod, E.; Givant, J.; Shappir, Y.; Feldman, Y.; Sa'ar, A. *Phys. Rev. B* **2006**, *65*, 165429.
- (21) Pitarke, J. M.; García-Vidal, F. J.; *Phys. Rev. B* **2001**, *63*, 073404. García-Vidal, F. J.; Pitarke, J. M.; Pendry, J. B. *Phys. Rev. Lett.* **1997**, *89*, 4289.

NL0710598